LETTERS
PUBLISHED ONLINE: 14 OCTOBER 2012 | DOI: 10.1038/NMAT3443

nature materials

Nanometre optical coatings based on strong interference effects in highly absorbing media

Mikhail A. Kats, Romain Blanchard, Patrice Genevet and Federico Capasso*

Optical coatings, which consist of one or more films of dielectric or metallic materials, are widely used in applications ranging from mirrors to eyeglasses and photography lenses[1,2]. Many conventional dielectric coatings rely on Fabry–Perot-type interference, involving multiple optical passes through transparent layers with thicknesses of the order of the wavelength to achieve functionalities such as anti-reflection, high-reflection and dichroism. Highly absorbing dielectrics are typically not used because it is generally accepted that light propagation through such media destroys interference effects. We show that under appropriate conditions interference can instead persist in ultrathin, highly absorbing films of a few to tens of nanometres in thickness, and demonstrate a new type of optical coating comprising such a film on a metallic substrate, which selectively absorbs various frequency ranges of the incident light. These coatings have a low sensitivity to the angle of incidence and require minimal amounts of absorbing material that can be as thin as 5–20 nm for visible light. This technology has the potential for a variety of applications from ultrathin photodetectors and solar cells to optical filters, to labelling, and even the visual arts and jewellery.

Optical coatings are a key component of nearly every optical device, and have been extensively studied for decades[1,2]. Conventional coatings comprise some combination of thin metallic films serving as partial and full reflectors, and wavelength-scale-thick dielectric films that rely on Fabry–Perot-type or thin-film interference—the same effect that is responsible for the colourful patterns on oil films and soap bubbles and for Newton's rings. Other examples include anti-reflection and high-reflection coatings, which are often made by stacking layers of dielectrics with quarter-wave thickness ($\lambda/4n$, where n is the refractive index of the material). These interference effects rely on multi-pass light circulation within the optical cavities formed by the films, and are typically sensitive to the angle of incidence. By engineering multi-layer dielectric stacks, more complex and robust devices such as omni-directional reflectors can be created[3]. Today, optical coatings, which often comprise many aperiodic layers, are primarily designed and optimized by computer software[4]; a variety of commercial software for thin-film calculation and optimization is available, including Essential Macleod, FilmStar, Film Wizard and OptiLayer.

Here, we explore the use of highly absorptive dielectric films as optical coatings. The Fabry–Perot-type effect of conventional optical thin films uses constructive and destructive interference, with the optical phase controlled by gradual accumulation within the nearly transparent dielectric layers. The material losses in the dielectrics are usually assumed to be small such that light is absorbed gradually, if at all, and the interface reflection and transmission phase changes at the interfaces between the dielectric films can therefore be assumed to be either 0 or π, depending on the index contrast. Our approach instead uses highly absorbing dielectrics (semiconductors at photon energies above the bandgap in the present demonstration) in which light is rapidly attenuated, together with metals that have finite optical conductivity. Combining these materials gives access to a range of interface reflection and transmission phase shifts that can be engineered by modification of the material properties. The large optical attenuation within the highly absorbing dielectrics and the concomitant non-trivial interface phase shifts lead to strong resonant behaviour in films that are much thinner than the wavelength of light. We demonstrate these ultrathin coatings on the surfaces of noble metals in the visible regime and show that deposition of nanometres of a lossy dielectric on a metal results in a marked modification of the reflectivity spectrum (and therefore colour).

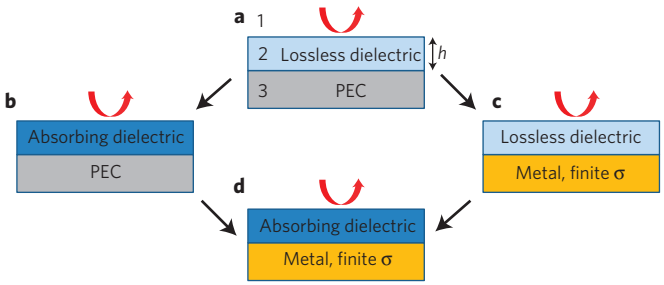

Figure 1 | Schematic of incident light from medium 1 (air) being reflected from a structure comprising dielectric medium 2 with thickness *h* and metallic medium 3. a, The case of a perfect electric conductor (PEC) and a lossless dielectric. As there is no absorption and no penetration into the metal, the reflectivity equals unity at all wavelengths. Structures approaching this limit can be used as phase-shifting elements, which are known as Gires–Tournois etalons. **b**, An absorbing dielectric on a PEC substrate supports an absorption resonance for $h \sim m\lambda/4n_2$ assuming that the losses (k_2) are relatively small and m is an odd integer. No resonance exists for h smaller than $\lambda/4n_2$. **c**, A lossless dielectric on a substrate with finite optical conductivity (for example, Au at visible frequencies) can support a resonance for $h \ll \lambda/4n_2$ owing to the non-trivial phase shifts at the interface between medium 2 and medium 3, but the total absorption is small because the only loss mechanism is the one associated with the finite reflectivity of the metal. **d**, An ultrathin ($h \ll \lambda/4n_2$) absorbing dielectric on Au at visible frequencies can support a strong and widely tailorable absorption resonance.

The equations describing the behaviour of light incident from air ($n_1 = 1$) onto a lossy film with thickness h and complex refractive index $\tilde{n}_2 = n_2 + ik_2$, deposited on a metallic substrate

School of Engineering and Applied Sciences, Harvard University, Cambridge, Massachusetts 02138, USA. *e-mail: capasso@seas.harvard.edu.

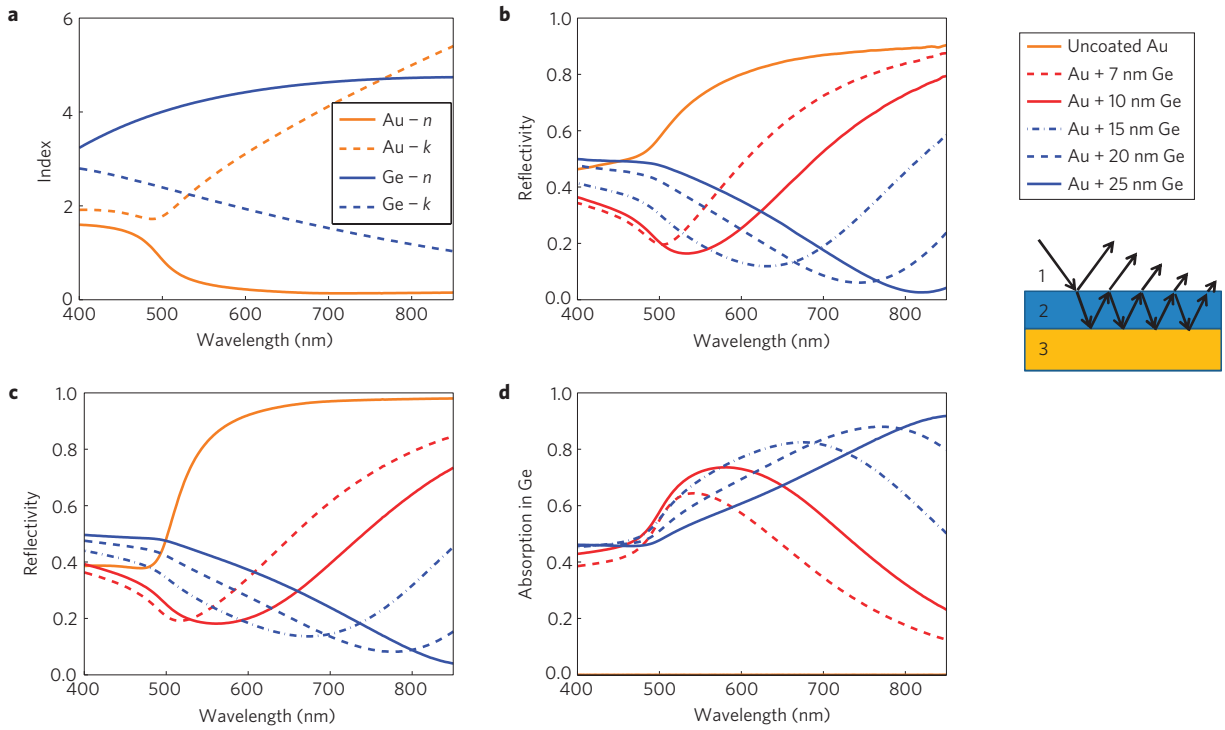

Figure 2 | Optical properties of the thin films. a, Real and imaginary parts of the complex refractive indices of Au and Ge, obtained by variable-angle spectroscopic ellipsometry. **b**, Near-normal incidence (7°) reflection spectra of thick Au coated with 7, 10, 15, 20 and 25 nm of Ge. Inset: schematic of the Ge film on a Au substrate, showing a partial wave decomposition. **c**, Calculated reflection spectra using equation (1) and the optical constants in **a** corresponding to the measurement in **b**. **d**, Calculated fraction of the total incident light that is absorbed within the Ge layer.

with complex index $\tilde{n}_3$ (Fig. 1), can be found in optics textbooks[5]. The reflection coefficient for transverse-electric (s-polarized) light incident at an angle θ_1 is

$$\tilde{r} = \frac{\tilde{r}_{12} + \tilde{r}_{23} e^{2i\tilde{\beta}}}{1 + \tilde{r}_{12}\tilde{r}_{23} e^{2i\tilde{\beta}}} \quad (1)$$

where $\tilde{r}_{mn} = (\tilde{p}_m - \tilde{p}_n)/(\tilde{p}_m + \tilde{p}_n)$, $\tilde{p}_m = \tilde{n}_m \cos(\tilde{\theta}_m)$, $\tilde{\beta} = (2\pi/\lambda)\tilde{n}_2 h \cos(\tilde{\theta}_2)$ and $\tilde{\theta}_m = \sin^{-1}(\sin(\theta_1)/\tilde{n}_m)$, which is the complex-valued form of Snell's law (pp. 740–741 of ref. 5). For transverse-magnetic (p-polarized) light, $\tilde{p}_m$ is replaced by $\tilde{q}_m = \cos(\tilde{\theta}_m)/\tilde{n}_m$. The total reflectivity is given by $R = |\tilde{r}|^2$, and because we assume that the substrate is metallic such that there is no transmission, the absorption of the structure can be written as $A = 1 - R$. One noteworthy special case of this three-layer structure is an asymmetric Fabry–Perot cavity comprising a quarter-wave film (or odd multiples thereof, such that $h \simeq m\lambda/4n_2$, where m is an odd integer) on a perfect reflector (Fig. 1a). This resonator in the presence of moderate losses serves as an absorbing optical cavity in which the loss can be considered as a perturbation. In the absence of loss, this type of cavity functions as a phase-shifting element called a Gires–Tournois etalon[6]. Asymmetric Fabry–Perot cavities have been used for reflection modulation[7], resonant cavity-enhanced photodetection and emission[8,9], ferroelectric infrared detection[10] and other applications.

For a metal substrate in the perfect electric conductor (PEC) limit, $n_3 \to \infty$ and $k_3 \to \infty$, so $\tilde{r}_{2,3} = -1$, corresponding to complete reflection with a phase shift of π (Fig. 1a,b), which makes $h \simeq \lambda/4n_2$ the lower limit on the thickness of a resonant cavity because a round trip inside such a cavity should accumulate approximately 0 phase (modulo 2π; see Supplementary Information for details). At optical frequencies, however, metals have finite conductivity and therefore their complex index is finite[5] (similar metal-like complex indices can also be found in a variety of non-metallic materials at longer wavelengths such as, for example, indium tin oxide in the near-infrared region[11], sapphire in the mid-infrared region[12] and so on), so the reflection phase shift at the metal interface can vary (Fig. 1c). Likewise, if a dielectric film has large optical losses (k_2 of the order of n_2), the reflection and transmission phase shifts at the boundary between it and air are not limited to 0 or π as in the case for lossless dielectrics (Fig. 1b,d). These non-trivial interface phase shifts allow the total phase accumulation, which includes both the interface and propagation phase shifts, to reach approximately 0 (modulo 2π) for certain films with thicknesses significantly below $\lambda/4n_2$, creating an absorption resonance (note that the phase accumulation is close to but not precisely zero at this resonance condition when the system has high losses). As there is very little light propagation in such a thin structure, the material optical losses must be very high for the round-trip absorption to be significant. By combining these non-trivial interface phase shifts, the phase accumulated through propagation and the attenuation of the wave as it propagates through the highly lossy medium, a new type of optical coating can be designed (Fig. 1d) where losses are no longer considered as a perturbation but are an integral part of the design.

We demonstrated these concepts at visible frequencies by modifying the reflectivity of a gold (Au) surface by coating it with evaporated germanium (Ge) films of a few nanometres in thickness, which creates broadband absorption resonances with the spectral position determined by the film thickness. The wide optical absorption band influences the colour by suppressing the reflectivity in a portion of the visible spectrum. Ge was selected because it is highly absorbing at visible frequencies (see Fig. 2a) owing to direct electronic transitions that appear at energies higher than that of the L-absorption edge[13]. We coated an optically thick (150 nm) Au film with Ge of thickness h between 7 and 25 nm by using electron-beam evaporation, which resulted in marked changes in the reflectivity. We performed near-normal

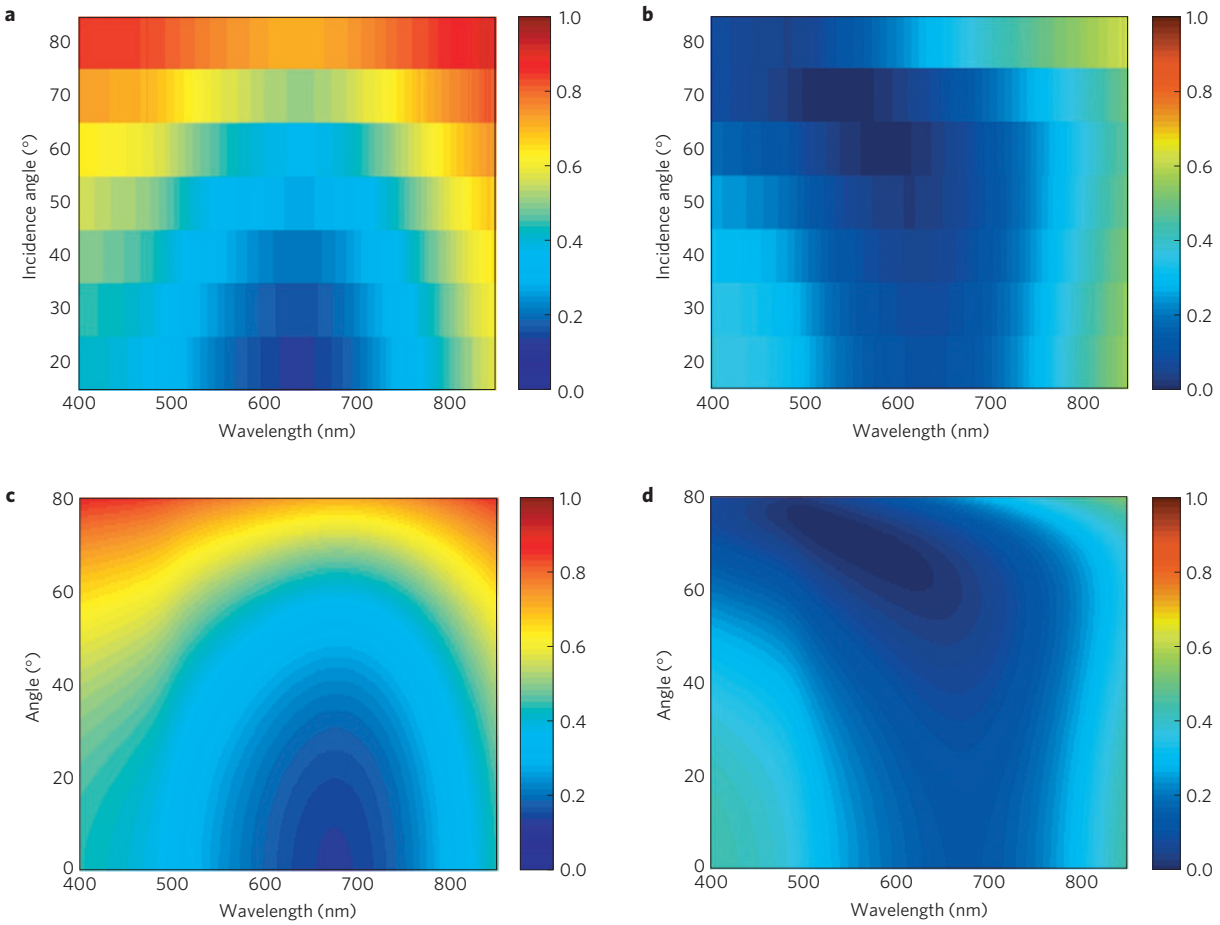

Figure 3 | Reflectivity spectra. a,**b**, Experimental reflectivity spectra for s- and p-polarization, respectively, for angles of incidence from 20° to 80° for an Au film coated with 15 nm of Ge (the value of reflectivity is indicated by the colour bars). **c**,**d**, The calculated spectra corresponding to those in **a**,**b** using equation (1).

incidence measurements (7° incidence angle with unpolarized light) between 400 and 850 nm using a spectrophotometer (see Methods and Supplementary Information for details on the sample preparation and measurement). The experimental reflectivity spectra for Ge films of thickness between 7 and 25 nm coated on Au are given in Fig. 2b.

The calculated reflection spectra corresponding to the measurements in Fig. 2b are obtained by using equation (1), and are shown in Fig. 2c. Excellent agreement is obtained between the experimental data and the calculations. The optical constants for the evaporated Au and Ge were obtained by variable-angle spectroscopic ellipsometry of optically thick films (see Supplementary Information for more details). We also computed the total fraction of the incident light that is absorbed within the Ge film (Fig. 2d), finding that most of the absorption occurs in this layer as opposed to the underlying Au. For example, in the case of the 15 nm Ge sample at a wavelength of ~670 nm, over 80% of the incident light is absorbed in the Ge layer whereas only ~4% of the light is absorbed in the Au, with the remaining ~15% of the light reflected. The spectral position of the absorption band, which corresponds to the reflectivity minimum, depends on h, with a shift of approximately 20 nm in wavelength for every 1 nm change in h across the visible spectral range. This strong absorption resonance occurs in a film that is much thinner than the wavelength of light (for example, $h \sim \lambda/(13n_2)$ at $\lambda \sim 560$ nm, with $n_2 \sim 4.3$ for the 10 nm Ge film in the calculation)—a result of the interplay between the complex reflection coefficient at the Ge/Au substrate and the large but finite attenuation of light within the Ge film (see Supplementary Information for a detailed explanation based on decomposition into partial waves). Note that in our material system, the absorption coefficient of Ge decreases with increasing wavelength and the properties of Au slowly approach those of a PEC, so the resonant absorption thickness will slowly converge to $h \sim \lambda/(4n_2)$ at long wavelengths.

As these coatings are much thinner than the wavelength of light, there is little phase accumulation due to the propagation through the film compared with the reflection phase change on reflection. As a result, the optical properties of these coatings are robust with respect to the angle of incidence. We demonstrated this by measuring the s- and p-polarized reflectivity of the sample with 15 nm of Ge, which shows that the absorption feature remains prominent for angles of incidence from 0° to ~60° in both polarizations (Fig. 3a,b). The corresponding calculated spectra are shown in Fig. 3c,d.

The large change in reflectivity allows for the colouring of metals using these films of subwavelength thickness. Figure 4 shows a photograph of samples of Au coated with Ge from 0 to 25 nm in thickness, creating a spectrum of colours including pink, blue and violet. In samples a–h, the substrate material for Au deposition was a polished silicon wafer. In samples i–k, however, the rough, unpolished back-side of the wafer was used, and the various colours are still clearly visible, indicating that the present effect is relatively insensitive to surface roughness. This is to be expected given the small dependence of the reflectivity on the incidence angle shown in Fig. 3, but runs against intuition given our everyday experience with thin-film interference effects. We also show several samples of

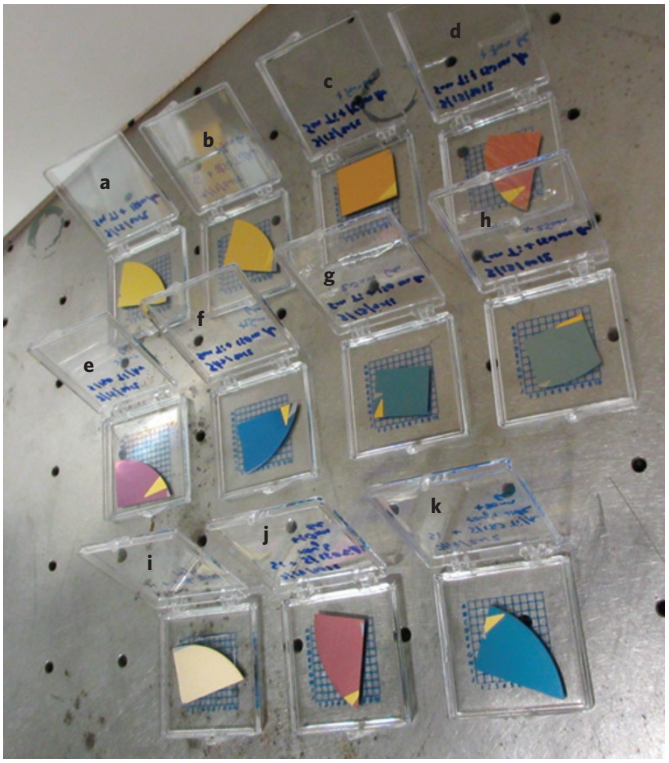

Figure 4 | Wide variety of colours formed by coating Au with nanometre films of Ge. a–h, 0, 3, 5, 7, 10, 15, 20 and 25 nm of Ge deposited on optically thick Au, which was deposited on polished silicon. The clip marks from mounting in the electron-beam evaporator are visible. **i–k**, 0, 10 and 20 nm of Ge deposited over 150 nm of Au, on a rough (unpolished) silicon substrate.

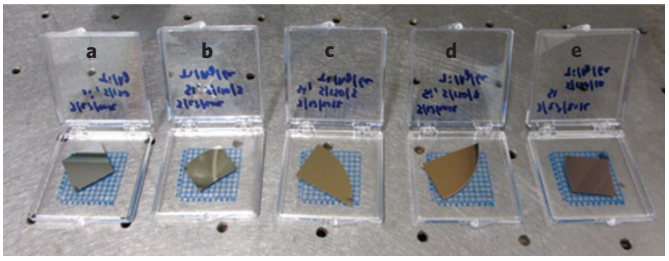

Figure 5 | Spectrum of colours resulting from coating Ag with nanometre films of Ge. a–e, Thick Ag films coated with 0, 3, 5, 7 and 10 nm of evaporated Ge, respectively.

silver (Ag) coloured using the same principle (Fig. 5); in particular, a colour similar to that of Au is induced in Ag samples by coating them with ~7 nm of Ge (Fig. 5d).

We note that the modification of the absorption and colour of metals has recently been demonstrated using nano-, micro- and macrostructuring of the metal surface by lithography and etching, femtosecond laser ablation or other methods[14–18]. By comparison, our technique is non-damaging to the metal surface, can be reversed by chemical etching of the absorbing dielectric layer, does not require any serial fabrication steps and involves only smooth surfaces, which may be advantageous for integration into devices. Furthermore, the approach demonstrated here does not involve multiple scattering, metallic nanocavity resonances or surface plasmons, as in refs 14–18, but is instead a result of simple, albeit counterintuitive, thin-film interference; this simplicity allows for the prediction and design of new coatings using simple analytical expressions such as equation (1).

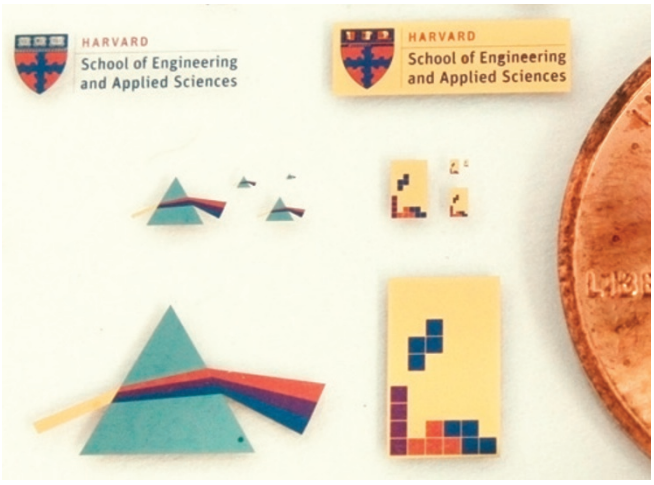

Figure 6 | Photograph of colour images generated using multi-step patterning of ultrathin Ge films, with the edge of a United States penny included for size comparison. Five steps of photolithography with alignment are used to selectively deposit an optically thick layer of Au on a glass slide, followed by Ge layers of either 7, 11, 15 or 25 nm. This yields light pink, purple, dark blue and light blue colours, respectively. Among the demonstrated patterns are the logo and shield of the School of Engineering and Applied Sciences; these are a trademark of Harvard University, and are protected by copyright; they are used in this research with permission.

In addition to continuous coatings, single- and multicolour images can be created by combining the deposition of ultrathin absorbing films with conventional lithographic techniques. As an example, we generated several colour images on a glass slide with feature sizes ranging from micrometres to millimetres by using multi-step contact photolithography with alignment (Fig. 6). Five colours are demonstrated: Au (0 nm of Ge), light pink (~7 nm), purple (~11 nm), dark blue (~15 nm) and light blue (~25 nm).

The approach of using ultrathin, absorptive dielectric films as optical coatings is very general and can be applied to applications across a range of frequencies, starting with simple absorbers and colour filters. The large change in optical properties given relatively small changes in material thickness can be used for subnanometre optical thickness monitoring of the deposition of semiconductor films. The colouring of metals with nanometre-thick films of inexpensive material may prove useful in various aspects of design and the visual arts. Furthermore, creating patterned structures comprising ultrathin absorbing coatings using conventional fabrication techniques introduces new capabilities for labelling, printing and otherwise displaying information.

The high degree of absorption in semiconductors makes them excellent candidate materials for these ultrathin coatings, potentially enabling new types of photodetectors with enhanced quantum efficiency that require orders of magnitude less semiconductor material, significantly decreasing the material cost and growth time (compared with, for example, resonant-cavity-enhanced photodetectors that have an absorbing layer inside a wavelength-scale Fabry–Perot cavity). Solar cell applications could also benefit from the large spectral bandwidth of the absorption resonances. Furthermore, in solar cells there is a tradeoff between thickness and material purity that is related to charge carrier lifetimes in materials with defects[19]; making ultrathin highly absorbing layers could relax this purity constraint, further reducing costs. Finally, when applied at infrared, millimetre and longer wavelengths, absorbing coatings backed by a reflector can be components of bolometer-type detectors and stealth technology.

Methods

The Au, Ge and Ag films were deposited by electron-beam evaporation using a Denton evaporator. Au was deposited at a rate of ~2 Å s^{-1} under a pressure of ~10^{-6} torr without substrate heating, with the rate measured by a crystal monitor. Ge was deposited at a rate of 1 Å s^{-1} at a pressure of ~2×10^{-6} torr. The images in Figs 4 and 5 were taken with a Canon PowerShot ELPH 310 HS digital camera under illumination from regular white ceiling fluorescent lights.

The near-normal incidence reflectivity spectra were taken using a Hitachi 4100 spectrophotometer with a tungsten lamp source and a photomultiplier tube in the 400–850 nm range. The angle-dependent, polarization-dependent spectra were obtained using a Woollam WVASE32 spectroscopic ellipsometer using reflection/transmission mode. The stability of these optical coatings is discussed in the Supplementary Information.

The complex refractive indices given in Fig. 2a and used in the calculation of the spectra in Figs 2c and 3c,d were obtained by variable-angle spectroscopic ellipsometry of optically thick evaporated films (150 nm for Au and 1,000 nm for Ge in the 400–850 nm range). In ellipsometry literature, this sort of measurement is referred to as measuring the pseudo-dielectric function, which is named pseudo because of the assumption that a single reflection comes from a sharp interface between the material and the air[20]. We preferred this method to ellipsometry on thin absorbing films (for example, ~10 nm Ge on a known substrate) because it decreases the number of unknowns from (n, k, h) to (n, k), which helps avoid over-fitting errors and non-unique solutions.

The theoretical spectra in Figs 2c and 3c,d were calculated using equation (1). In the case of Fig. 2c, we simulated unpolarized incident light by calculating the reflectivity for both s- and p-polarizations, and taking an average of the two.

The multicolour patterns of Fig. 6 were generated by five steps of contact photolithography with alignment. Photoresist was spun onto a glass slide (Shipley S1813, 4,000 r.p.m.), was exposed through chrome-coated glass photomasks using a Karl Suss MJB4 mask aligner and was then developed using CD-26. The Au and Ge films were then deposited through the resulting mask, with the excess material removed using liftoff in acetone with ultrasonic agitation. The deposition thicknesses were 65 nm Au (preceded by a 5 nm Ti adhesion layer) to create an optically thick layer, followed by 7 nm, 4 nm, 4 nm and 10 nm of Ge, creating overall Ge layers of thickness 7 nm, 11 nm, 15 nm and 25 nm, respectively.

Received 20 June 2012; accepted 31 August 2012; published online 14 October 2012

References

1. Macleod, H. A. *Thin-film Optical Filters* (Adam Hilger, 1986).
2. Yeh, P. *Optical Waves in Layered Media* (Wiley, 2005).
3. Fink, Y. *et al.* A dielectric omnidirectional reflector. *Science* **282,** 1679–1682 (1998).
4. Dobrowolski, J. A. Versatile computer program for absorbing optical thin film systems. *Appl. Opt.* **20,** 74–81 (1981).
5. Born, M & Wolf, E *Principles of Optics* 7th edn (Cambridge Univ. Press, 2003).
6. Gires, F. & Tournois, P. Interferometre utilisable pour la compression d'impulsions lumineuses modulees en frequence. *C. R. Acad. Sci. Paris* **258,** 6112–6615 (1964).
7. Yan, R. H., Simes, R. J. & Coldren, L. A. Electroabsorptive Fabry–Perot reflection modulators with asymmetric mirrors. *IEEE Photon. Technol. Lett.* **1,** 273–275 (1989).
8. Kishino, K., Selim Unlu, M., Chyi, J-I., Reed, J., Arsenault, L. & Morkoc, H. Resonant cavity-enhanced (RCE) photodetectors. *IEEE J. Quantum Electron.* **27,** 2025–2034 (1991).
9. Unlu, M. S. & Strite, S. Resonant cavity enhanced photonic devices. *J. Appl. Phys.* **78,** 607–639 (1995).
10. Bly, V. T. & Cox, J. T Infrared absorber for ferroelectric detectors. *Appl. Opt.* **33,** 26–30 (1994).
11. Robusto, P. F. & Braustein, R. Optical measurements of the surface plasmon of indium tin oxide. *Phys. Status Solidi* **119,** 155–168 (1990).
12. Gervais, F. & Piriou, B. Anharmonicity in several-polar-mode crystals: adjusting phonon self-energy of LO and TO modes in Al_2O_3 and TiO_2 to fit infrared reflectivity. *J. Phys. C* **7,** 2374–2386 (1974).
13. Cardona, M. & Harbeke, G. Absorption spectrum of germanium and zinc-blende-type materials at energies higher than the fundamental absorption edge. *J. Appl. Phys.* **34,** 813–818 (1963).
14. Zhang, J. *et al.* Continuous metal plasmonic frequency selective surfaces. *Opt. Express* **19,** 23279–23285 (2011).
15. Vorobyev, A. Y. & Guo, C. Enhanced absorptance of gold following multipulse femtosecond laser ablation. *Phys. Rev. B* **72,** 195422 (2005).
16. Vorobyev, A. Y. & Guo, C. Colorizing metals with femtosecond laser pulses. *Appl. Phys. Lett.* **92,** 041914 (2008).
17. Wang, X., Zhang, D., Zhang, H., Ma, Y. & Jiang, J. Z. Tuning color by pore depth of metal-coated porous alumina. *Nanotechnology* **22,** 305206 (2011).
18. Chattopadhyay, S. *et al.* Anti-reflecting and photonic nanostructures. *Mater. Sci. Eng. R* **69,** 1–35 (2010).
19. Lewis, N. S. Toward cost-effective solar energy use. *Science* **315,** 798–801 (2007).
20. Hilfiker, J. N. *et al.* Survey of methods to characterize thin absorbing films with spectroscopic ellipsometry. *Thin Solid Films* **516,** 7979–7989 (2008).

Acknowledgements

We acknowledge helpful discussions with J. Lin, N. Yu and J. Choy, and thank J. Deng and R. Sher for assistance with the measurements. We also thank L. Liu and E. Grinnell for assistance in photography. The fabrication and some of the measurements were performed at the Harvard Center for Nanoscale Systems, which is a member of the National Nanotechnology Infrastructure Network. We thank E. Mazur for access to his spectrophotometer. This research is supported in part by the Air Force Office of Scientific Research under grant number FA9550-12-1-0289. M. Kats is supported by the National Science Foundation through a Graduate Research Fellowship.

Author contributions

M.A.K. developed the concept, performed the calculations and fabricated the samples. M.A.K. and R.B. characterized the samples and performed the measurements. M.A.K., R.B., P.G. and F.C. analysed and interpreted the data and implications. M.A.K., R.B. and F.C. wrote the manuscript. F.C. supervised the research.

Additional information

Supplementary information is available in the online version of the paper. Reprints and permissions information is available online at www.nature.com/reprints. Correspondence and requests for materials should be addressed to F.C.

Competing financial interests

The authors declare no competing financial interests.